015115JCP = 015115JCP
Running Title: Electronic states of Si_2 and Si_2^-

Study of the low-lying electronic states of Si_2 and Si_2^- using negative ion photodetachment techniques

T. N. Kitsopoulos, C. J. Chick,[a] Y. Zhao, and D. M. Neumark[b]
Department of Chemistry, University of California, Berkeley, California 94720

(Received 22 March 1991; accepted 16 April 1991)

The low-lying electronic states of Si_2^- and Si_2 were studied using both photoelectron spectroscopy and threshold photodetachment spectroscopy of Si_2^-. Our measurements show that the ground state of Si_2 is the $X\,^3\Sigma_g^-$ state and that the $X\,^3\Sigma_g^- - D\,^3\Pi_u$ splitting is 0.083 ± 0.010 eV. Additional spectroscopic constants for the $X\,^3\Sigma_g^-$, $D\,^3\Pi_u$, $a\,^1\Delta_g$, $b\,^1\Pi_u$ and $c\,^1\Sigma_g^+$ states of Si_2 were also determined. For Si_2^-, the first two electronic states were identified as: $^2\Pi_u$ ($T_e = 0$, $r_e = 2.207 \pm 0.005$ Å, and $\nu = 533 \pm 5$ cm^{-1}) and $^2\Sigma_g^+$ ($T_e = 0.025 \pm 0.010$ eV, $r_e = 2.116 \pm 0.005$ Å, and $\nu = 528 \pm 10$ cm^{-1}). The electron affinity for Si_2 was found to be 2.176 ± 0.002 eV. Our results provide definitive orderings and splittings for the low-lying electronic states in both Si_2 and Si_2^-.

INTRODUCTION

The spectroscopy of elemental clusters has become the focus of much experimental and theoretical research in recent years.[1-4] A primary goal of these studies is to determine how chemical bonding in a cluster evolves as the number of atoms is varied. A full understanding of bonding in a cluster requires the characterization not only of its ground electronic state, but also of its low-lying excited electronic states. This is a formidable challenge due to the likely presence of a large number of low-lying electronic states in a many-atom cluster.[5-8] As a first step towards understanding the nature of electronic states in larger clusters, we report here the results of two types of photodetachment experiments on Si_2^- which yield a detailed picture of the low-lying electronic states of Si_2 as well as the lowest two electronic states of Si_2^-.

The electronic structure of Si_2 is complex. It has three low-lying molecular orbital configurations: $(3p)\sigma_g^2(3p)\pi_u^2$, $\sigma_g^1\pi_u^3$ and $\sigma_g^0\pi_u^4$. The two triplet and four singlet states arising from these configurations are shown in Fig. 1. *Ab initio* calculations predict the $X\,^3\Sigma_g^-$ ($\sigma_g^2\pi_u^2$) to be the ground state and the $D\,^3\Pi_u(\sigma_g^1\pi_u^3)$ state to lie only 20–100 meV above;[9-14] this interval is very sensitive to the level of the calculation. The $a\,^1\Delta_g$, $b\,^1\Pi_u$, and $c\,^1\Sigma_g^+$ singlet states are predicted to lie between 0.4–0.9 eV above the ground state, with the $d\,^1\Sigma_g^+$ state slightly higher (1.1–1.5 eV). Experimentally, electronic transitions originating from the $X\,^3\Sigma_g^-$ and $D\,^3\Pi_u$ states have been observed by several investigators,[15,16] but transitions between the two states have not been seen. The only previous experimental value of the D–X splitting, 53 ± 15 meV, was obtained from the Si_2^- photoelectron spectroscopy work of Ellison and co-workers.[17] Within the singlet manifold, absorption bands originating from the $c\,^1\Sigma_g^+$ state have been observed,[18] and an emission band due to the $d\,^1\Sigma_g^+ - b\,^1\Pi_u$ transition has been seen.[19] However, prior to the work reported here, the $a\,^1\Delta_g$ state had not been observed, the energy of the $c\,^1\Sigma_g^+$ state relative to the other low-lying singlet states was not known, and the energy of the entire manifold of singlet states relative to the triplet manifold had not been determined.

The silicon dimer anion Si_2^- also has two low-lying electronic states: the $^2\Sigma_g^+$ state from the $\sigma_g\pi_u^4$ configuration and the $^2\Pi_u$ state from the $\sigma_g^2\pi_u^3$ configuration. *Ab initio* calculations predict these states to be nearly degenerate.[20,21] If we assume that the ground electronic state Si_2^- results from adding one electron to the LUMO of the $X\,^3\Sigma_g^-$ state of the Si_2 (the π_u molecular orbital), we would expect the $^2\Pi_u$ to be the ground state. Again, the only prior experimental probe of this splitting is Ellison's Si_2^- photoelectron spectrum;[17] from his analysis, he concluded that the $^2\Pi_u$ state is the ground state and the $^2\Sigma_g^+ - {}^2\Pi_u$ splitting is 117 ± 16 meV.

In order to sort out the electronic states in Si_2^- and Si_2, we have studied Si_2^- using two forms of photodetachment spectroscopy: fixed-frequency photoelectron spectroscopy and threshold photodetachment spectroscopy. Negative ion photodetachment is a powerful method for studying clusters[22-26] since one can easily mass-select the species of interest prior to spectroscopic investigation. In addition, since the selection rules for photodetachment are different from those of optical spectroscopy, one can probe electronic states that are "dark" (forbidden) in emission or absorption experiments.[27] In particular, all of the Si_2 electronic states in Fig. 1 are accessible from either the $^2\Pi_u$ or $^2\Sigma_g^+$ states of Si_2^-. The combination of the two experiments is quite powerful. Although the energy resolution of the threshold photodetachment spectrometer is considerably higher than that of the photoelectron spectrometer, not all of the allowed photodetachment transitions are observed in the threshold spectrometer (see below).

The two experiments have enabled us to determine the energies of the six Si_2 electronic states in Fig. 1, as well as the splitting between the two low-lying electronic states of the anion. We find that the $X\,^3\Sigma_g^-$ and $^2\Pi_u$ states are indeed the

[a] NSF Predoctoral Fellow.
[b] NSF Presidential Young Investigator and Alfred P. Sloan Fellow.

 0021-9606/91/151441-08$03.00

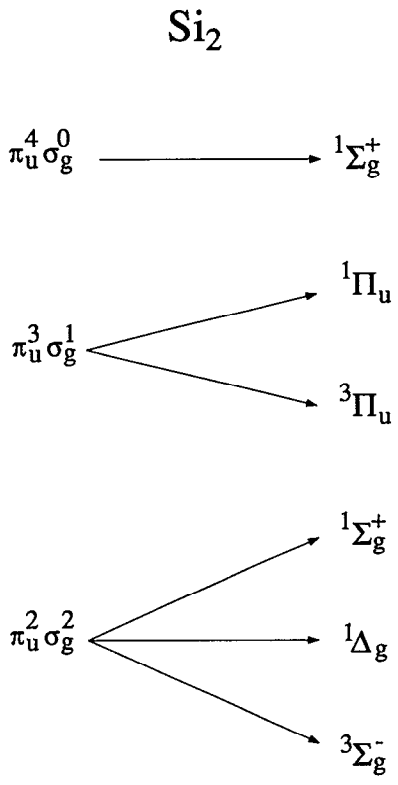

FIG. 1. The six low-lying electronic states resulting from the three possible valence orbital configurations of Si_2.

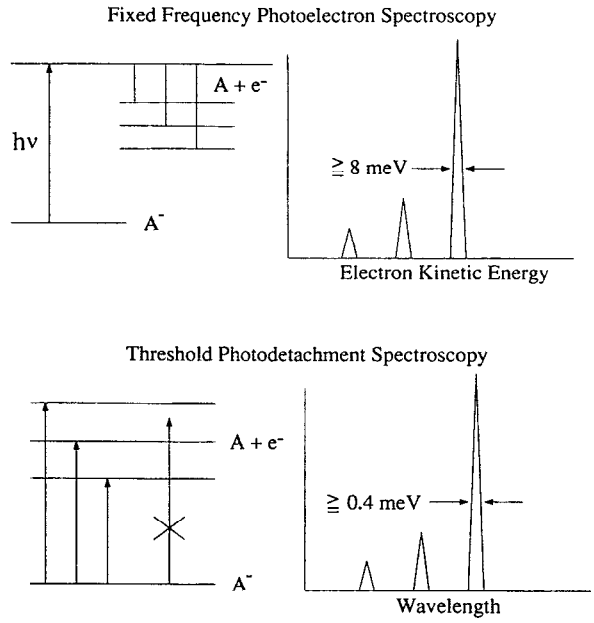

FIG. 2. Detection schemes for the fixed frequency photoelectron spectrometer and the threshold photodetachment spectrometer.

ground states of Si_2 and Si_2^-, respectively. The $D\,^3\Pi_u - X\,^3\Sigma_g^-$ interval in Si_2 is 83 ± 10 meV, and the $^2\Sigma_g^+ - ^2\Pi_u$ interval in Si_2^- is 24 ± 10 meV. In addition, we determined spectroscopic constants (vibrational frequencies, bond lengths and spin orbit splittings) for both the triplet and singlet states of Si_2, as well as for the $^2\Sigma_g^+$ and $^2\Pi_u$ states of Si_2^-.

EXPERIMENT

Two instruments were used in this study: a time-of-flight (TOF) photoelectron spectrometer[28] and a threshold photodetachment spectrometer.[29] In both instruments, Si_2^- anions are generated by laser vaporization. The anions are mass selected in a time-of-flight mass spectrometer. The anion of interest is subsequently photodetached and the resulting photoelectrons are detected using one of the schemes illustrated in Fig. 2 and described in more detail below.

The silicon negative ion clusters in both spectrometers are generated with a laser vaporization/pulsed molecular beam source.[30] The output of a XeCl excimer laser (308 nm, 5–15 mJ/pulse) is focused onto the surface of a rotating and translating silicon rod. The resulting plasma is entrained in a pulse of He from a pulsed solenoid valve (0.05 cm diameter orifice), and expanded through a "clustering channel" into the source vacuum chamber. This arrangement produces negative ions in sufficient quantity directly; no further means of attaching electrons to neutral clusters is needed.

In the photoelectron spectrometer, a Wiley–McLaren time-of-flight mass spectrometer is used for mass separation.[31] The anions are extracted from the source region by applying a pulsed 100 V/cm field perpendicular to the molecular beam axis. The anions are accelerated to 1000 eV, and the ions separated into bunches according to mass as they traverse a 140 cm flight tube. In the threshold photodetachment spectrometer, the cluster beam passes through a 2 mm skimmer into a lower pressure, differentially pumped region before any acceleration occurs. The anions are accelerated to 1000 eV and mass selected using a time-of-flight mass spectrometer based on Bakker's design.[32] Based on the observed "hot bands" (see below), the anions produced in the threshold spectrometer source were colder than in the photoelectron spectrometer source. This may have resulted from not applying any acceleration fields in the relatively high pressure source region in the threshold spectrometer, but may also be due to slightly different source operating conditions used in the two instruments.

In the photoelectron spectrometer, the mass-selected Si_2^- anions are photodetached with a fixed-frequency pulsed laser. A small fraction (10^{-4} of the ejected photoelectrons are collected at the end of a 100 cm field-free flight tube and are energy-analyzed by time of flight. The electron kinetic energy distribution yields the transition energies between the anion and neutral (Fig. 2, top). The energy resolution of this instrument is 8 meV (64 cm^{-1}) for electrons with 0.65 eV kinetic energy and degrades as $(KE)^{3/2}$.[3/2] This is sufficient to resolve vibrational features in the photoelectron spectrum. The spectra here were obtained with the third harmonic of a Nd:YAG laser at 355 nm, 20 Hz repetition rate and each spectrum was signal averaged for 80 000 laser shots. Spectra were obtained at two polarization angles, $\theta = 0°$ and 90°, where θ is the angle between the electric vector of the laser light and the direction of electron detection.

In the threshold photodetachment spectrometer, Si_2^-

was photodetached using an excimer-pumped tunable dye laser operating at 50 Hz. Only those photoelectrons with nearly zero kinetic energy are collected (Fig. 2, bottom). In principle, this yields the same information as photoelectron spectroscopy. However, the energy resolution is considerably higher. This particular threshold electron detection scheme was developed by Müller–Dethlefs *et al.* for neutral photoionization.[33] Our implementation of this to threshold photodetachment of anions has been described previously.[29] Gantefor *et al.*[34] have recently used threshold photodetachment to study Au_2^-. The resolution of our instrument is 3 cm^{-1} at best, but for optimum signal to noise, the threshold spectra in this work were obtained at an estimated resolution of 15 cm^{-1}. At this resolution, we observe spin–orbit fine structure in addition to vibrational structure, but individual rotational transitions are not resolved.

The threshold spectra were signal averaged for 1000 laser shots at each laser frequency. In order to probe the spectral region of interest (435 to 595 nm), four different laser dyes were used: Coumarin 440 (423–460 nm), Coumarin 460 (440–480 nm), Coumarin 540 (530–580 nm), and Rhodamine 6G (580–600 nm).

RESULTS

Our photoelectron spectra obtained at 355 nm ($h\nu = 3.49$ eV) and $\theta = 0°$ and 90° are presented in Figs. 3 and 4.[35] The electron kinetic energy (eKE) is related to the internal (vibrational + electronic) energy of the anion $E^{(-)}$ and the neutral $E^{(0)}$ by

$$eKE = h\nu - EA - E^{(0)} + E^{(-)},$$

where EA is the electron affinity of the neutral ground state. Peaks A–F are in the same energy range as the peaks seen by Ellison[17] and correspond to transitions to the triplet states of Si_2, while peaks G–L are due to transitions to higher lying singlet states.

Figures 3 and 4 show that varying the laser polarization changes the peak intensities in different ways. Peaks D and E are more intense at $\theta = 0°$ than at 90°, peaks B, C, and F are relatively insensitive to the laser polarization, while peaks d and e are not evident in the $\theta = 0°$ spectrum. The singlet band also shows three types of peaks. Peaks G, H and J have maximum intensity at $\theta = 0°$, I and K are most intense at $\theta = 90°$, and peak L has the same intensity in both polarizations. In Ellison's spectrum a lower photon energy was used (2.54 eV) and thus only four peaks (A–D) were observed. In addition, the D, d doublet in Fig. 4 was not resolved.

The threshold photodetachment spectra are shown in Figs. 5 and 6. Several of the peaks in the photoelectron spectra appear as multiple peaks in the higher resolution threshold spectra. In the spectrum of Fig. 5, peak B becomes a doublet (B_1,B_2), while peak C splits into C_1 and C_2 along with additional weak peaks labeled c_1' and c_3'. In addition, peak d appears as three intense transitions (d_1,d_2,d_3) and a small peak c_2; peak e also becomes a triplet (e_1,e_2,e_3). Peaks D and E in the photoelectron spectra are absent from the threshold spectrum. The significance of this observation will be discussed below.

Similar effects are observed for the singlet band. Peaks G and H become doublets at higher resolution peak J remains a single peak, and peaks I and K are absent from the threshold spectrum. The peak positions for all the spectra are listed in Table I. In all the threshold spectra, the peak widths are about 40 cm^{-1} (5 meV). This is most likely a combination of instrumental resolution and broadening from unresolved rotational transitions.

DISCUSSION

In many small molecule photoelectron spectra, it is straightforward to distinguish transitions between different electronic states of the anion and neutral from vibrational progressions within a given electronic band.[36] However, the predicted spacings between several of the Si_2 and Si_2^- low-lying electronic states are comparable to the known and calculated vibrational frequencies, most of which are around 500 cm^{-1} (60 meV). Thus, the key to understanding the Si_2^- photoelectron spectra and threshold photodetachment spectra is to be able to sort out the overlapping electronic transitions and vibrational progressions in these spectra.

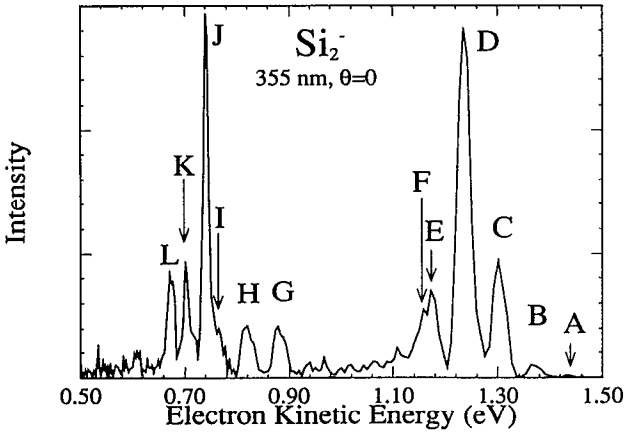

FIG. 3. Photoelectron spectrum of Si_2^- at 355 nm (3.49 eV), with laser polarization parallel to the direction of electron detection.

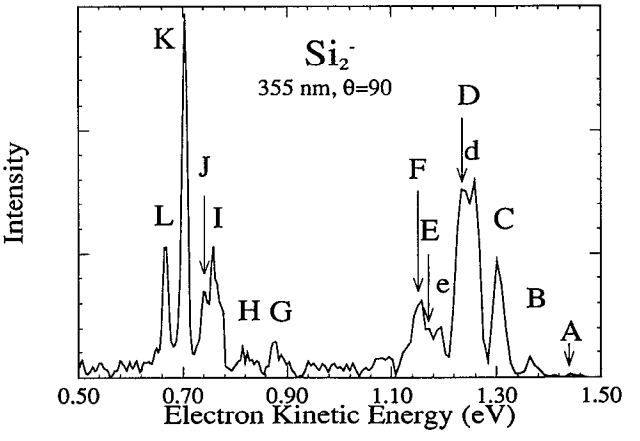

FIG. 4. Photoelectron spectrum of Si_2^- at 355 nm (3.49 eV), with laser polarization perpendicular to the direction of electron detection.

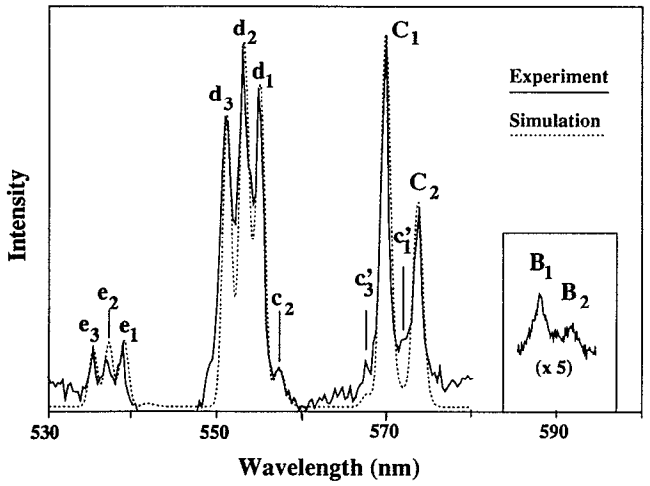

FIG. 5. Threshold photodetachment spectrum of Si_2^- showing the $X\,^3\Sigma_g^-$ $\leftarrow {}^2\Pi_u$ and $D\,^3\Pi_u \leftarrow {}^2\Sigma_g^+$ neutral $\leftarrow$ anion electronic transitions. In the simulated spectrum shown, the peak widths were set at 0.005 eV (40 cm^{-1}).

The polarization dependence of the peaks in a photoelectron spectrum[37] provides a means of distinguishing electronic from vibrational transitions. As described in the Results, the sets of peaks (B, C, F), (d, e), and (D, E) in the triplet region of the photoelectron spectra each have different angular distributions with respect to the electric field vector of the laser, suggesting that each set is due to a different neutral $\leftarrow$ anion electronic transition. The spacing between peaks d and e is identical to that between D and E (64 meV or 516 cm^{-1}), implying that each pair is a vibrational progression in the same electronic state of neutral Si_2. Similarly, in the singlet region, peaks (G,H,J), peaks (I,K), and peak L apparently arise from three different electronic transitions.

We now consider the transitions between Si_2^- and Si_2 electronic states that could contribute to the triplet region of the spectra. The experimental values of r_e, the equilibrium bond length, and ω_e, the harmonic vibrational frequency, are 2.246 Å and 511 cm^{-1} for the Si_2 $X\,^3\Sigma_g^-$ state and 2.155 Å, 539 cm^{-1} for the $D\,^3\Pi_u$ state.[15,38] Calculations by Bauschlicher[9] yield a $D\,^3\Pi_u$–$X\,^3\Sigma_g^-$ gap of 440 $\pm$ 100 cm^{-1} (55 $\pm$ 12 meV). Other calculations by Bruna[11] and McLean[12] predict splittings of 20 and 130 meV, respectively. In spite of the numerical disagreement surrounding this triplet gap, the consensus among theoreticians is that the $X\,^3\Sigma_g^-$ state is the ground state of the neutral dimer.

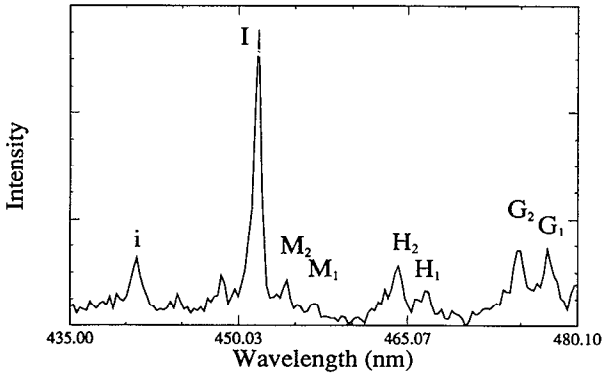

FIG. 6. The threshold photodetachment spectrum of Si_2^- showing the $a\,^1\Delta_g \leftarrow {}^2\Pi_u$ and $b\,^1\Pi_u \leftarrow {}^2\Sigma_g^+$ neutral $\leftarrow$ anion electronic transitions.

TABLE I. Peak positions and assignments for the photoelectron and threshold photodetachment spectra of Si_2^-. Peaks appearing only in the photoelectron spectra are marked with an asterisk (*) and their energy uncertainty is $\pm$ 0.010 eV. The energy uncertainty of all other peaks in the table is $\pm$ 0.001 eV.

Peak	Position (eV)	$Si_2 \leftarrow Si_2^-$
A*	2.052	$^3\Sigma_g^-(v'=0) \leftarrow {}^2\Pi_u(v''=2)$
B_2	2.095	$^3\Sigma_g^-(v'=0) \leftarrow {}^2\Pi_{1/2}(v''=1)$
B_1	2.109	$^3\Sigma_g^-(v'=0) \leftarrow {}^2\Pi_{3/2}(v''=1)$
C_2	2.161	$^3\Sigma_g^-(v'=0) \leftarrow {}^2\Pi_{1/2}(v''=0)$
c_1'	2.169	$^3\Pi_2(v'=0) \leftarrow {}^2\Sigma_g^+(v''=1)$
C_1	2.176	$^3\Sigma_g^-(v'=0) \leftarrow {}^2\Pi_{3/2}(v''=0)$
c_3'	2.185	$^3\Pi_0(v'=0) \leftarrow {}^2\Sigma_g^+(v''=1)$
c_2	2.225	$^3\Sigma_g^-(v'=1) \leftarrow {}^2\Pi_{1/2}(v''=0)$
d_1	2.235	$^3\Pi_2(v'=0) \leftarrow {}^2\Sigma_g^+(v''=0)$
d_2	2.242	$^3\Pi_1(v'=0) \leftarrow {}^2\Sigma_g^+(v''=0)$
d_3	2.250	$^3\Pi_0(v'=0) \leftarrow {}^2\Sigma_g^+(v''=0)$
D*	2.259	$^3\Pi_{0,1,2}(v'=0) \leftarrow {}^2\Pi_{1/2,3/2}(v''=0)$
e_1	2.301	$^3\Pi_2(v'=1) \leftarrow {}^2\Sigma_g^+(v''=0)$
e_2	2.309	$^3\Pi_1(v'=1) \leftarrow {}^2\Sigma_g^+(v''=0)$
e_3	2.316	$^3\Pi_0(v'=1) \leftarrow {}^2\Sigma_g^+(v''=0)$
E*	2.323	$^3\Pi_{0,1,2}(v'=1) \leftarrow {}^2\Pi_{1/2,3/2}(v''=0)$
F*	2.335	?
G_1	2.598	$^1\Delta_g(v'=0) \leftarrow {}^2\Pi_{1/2}(v''=0)$
G_2	2.611	$^1\Delta_g(v'=0) \leftarrow {}^2\Pi_{3/2}(v''=0)$
H_1	2.658	$^1\Delta_g(v'=1) \leftarrow {}^2\Pi_{1/2}(v''=0)$
H_2	2.672	$^1\Delta_g(v'=1) \leftarrow {}^2\Pi_{3/2}(v''=0)$
M_1	2.715	$^1\Delta_g(v'=2) \leftarrow {}^2\Pi_{1/2}(v''=0)$
M_2	2.724	$^1\Delta_g(v'=2) \leftarrow {}^2\Pi_{3/2}(v''=0)$
I	2.745	$^1\Pi_u(v'=0) \leftarrow {}^2\Sigma_g^+(v''=0)$
i	2.812	$^1\Pi_u(v'=1) \leftarrow {}^2\Sigma_g^+(v''=0)$
J*	2.753	$^1\Pi_u(v'=0) \leftarrow {}^2\Pi_{1/2,3/2}(v''=0)$
K*	2.789	$^1\Sigma_g^+(v=0) \leftarrow {}^2\Sigma_g^+(v''=0)$
L*	2.825	?

In a recent calculation by Raghavachari and Rohlfing[21] on Si_2^-, r_e and ω_e were found to be 2.124 Å and 579 cm^{-1} for the $^2\Sigma_g^+$ state and 2.202 Å, 539 cm^{-1} for the $^2\Pi_u$ state. They also found the $^2\Pi_u$ state to lie 43 meV below the $^2\Sigma_g^+$ state. However, as was the case in an earlier calculation by Bruna,[20] the splitting and even the ordering of these states is uncertain.

In Fig. 7, we have drawn an energy level diagram for the first two electronic states of the neutral and anion dimer. The ordering of the levels is based on the above *ab initio* results. In a typical photoelectron spectrum one only observes transitions between anion and neutral electronic states which involve removal of one electron (one-electron transitions). According to this rule, three of the four possible transitions among these states are allowed; only the $X\,^3\Sigma_g^- \leftarrow {}^2\Sigma_g^+$ transition is forbidden. The three allowed transitions are labeled

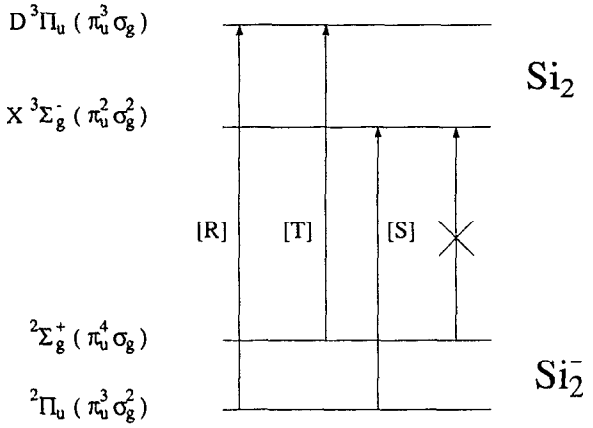

FIG. 7. Energy level diagram showing the one-electron transitions between the $^2\Pi_u$ and $^2\Sigma_g^+$ electronic states of Si_2^- and the triplet electronic states of Si_2.

[R], [S], [T] corresponding to the $D\,^3\Pi_u \leftarrow {}^2\Pi_u$, $X\,^3\Sigma_g^- \leftarrow {}^2\Pi_u$ and $D\,^3\Pi_u \leftarrow {}^2\Sigma_g^+$ transitions, respectively, where we have maintained the same notation used by Ellison.[17] Thus, Fig. 7 explains why three overlapping electronic transitions occur in the triplet region of the photoelectron spectrum. However, a unique identification of the peaks in the spectra with the three allowed transitions requires additional information obtained from the threshold photodetachment spectra.

The first point to consider is the reason why peaks D and E are absent from the threshold photodetachment spectra. The energy dependence of the photodetachment cross section near the threshold energy $E_{\rm th}$ for an neutral$\leftarrow$anion transition is described by Wigner's law,[39]

$$\sigma(E) \propto (E - E_{\rm th})^{l+1/2},$$

where l is the orbital angular momentum of the detached electron. For s-wave ($l=0$) detachment, the cross section goes as $(E-E_{\rm th})^{1/2}$ and is therefore quite large just above the threshold energy. However, for $l \geqslant 1$ (p-wave higher), $\sigma(E)$ is very small just above $E_{\rm th}$. In our threshold photodetachment spectrometer, only those photoelectrons produced a few cm^{-1} above a neutral$\leftarrow$anion transition are collected. Thus, only transitions that proceed via s-wave detachment are observed.

Reed *et al.*[40] have shown that one can predict if s-wave photodetachment can occur based on the symmetry of the molecular orbital in the anion from which photodetachment occurs. For Si_2^-, which has $D_{\infty h}$ symmetry, photodetachment from a π_u orbital can go by an s-wave near threshold, whereas s-wave photodetachment from a σ_g orbital is forbidden and only detachment via higher partial waves ($l \geqslant 1$) can occur. Figure 7 shows that the electronic transitions [S] and [T] involve the removal of a π_u electron and can therefore undergo s-wave photodetachment. On the other hand, in transition [R], a σ_g electron is ejected and s-wave detachment cannot occur. Hence, the *absence* of peaks D and E in the threshold photodetachment spectrum means they are due to the electronic transition [R], the $D\,^3\Pi_u \leftarrow {}^2\Pi_u$ transition. Peaks D and E are separated by $516 \pm 60\ cm^{-1}$ in the photoelectron spectra, which is characteristic of a vibrational frequency in either Si_2 or Si_2^-. The *ab initio* calculations discussed above predict a relatively small bond length change upon photodetachment, so the considerably greater intensity of peak D indicates it is the $v'=0 \leftarrow v''=0$ vibrational transition associated with the electronic transition [R], while E is the $1 \leftarrow 0$ vibrational transition.

We can now assign the peaks that appear in the threshold photodetachment spectra. Consider peaks d and e in the spectrum of Fig. 5. At the higher resolution in this spectrum, both peaks appear as triplets, with the peaks in each triplet evenly spaced by about $64 \pm 10\ cm^{-1}$. This compares well with the experimentally determined $71.6\ cm^{-1}$ splitting between the $^3\Pi_2$, $^3\Pi_1$, $^3\Pi_0$ spin–orbit components (listed in order of ascending energy) of the $^3\Pi_u$ electronic state.[15] This triplet pattern is expected for the $D\,^3\Pi_u \leftarrow {}^2\Sigma_g^+$ neutral$\leftarrow$anion transition, (the spin–rotation splitting in the $^2\Sigma_g^+$ will not be resolved in our spectra) and peaks d and e are assigned to this electronic transition ([T] in Fig. 7). The d_i–e_i separation is $530 \pm 10\ cm^{-1}$, and, based on the much greater intensity of d, peaks d and e are assigned to the $0 \leftarrow 0$ and $1 \leftarrow 0$ vibrational transitions associated with [T].

Peaks B and C each appear as doublets split by $122 \pm 10\ cm^{-1}$ in Fig. 5. The only unassigned neutral$\leftarrow$anion transition in Fig. 7 is [S], the $X\,^3\Sigma_g^- \leftarrow {}^2\Pi_u$ transition. This transition should yield doublets separated by the spin–orbit splitting between the $^2\Pi_{3/2}$ and $^2\Pi_{1/2}$ levels of the anion. We therefore assign peaks B and C to this transition and the observed $122\ cm^{-1}$ interval to the spin–orbit splitting in the anion $^2\Pi_u$ state. Based on the ordering of the $^3\Pi_u$ levels of Si_2, the $^2\Pi_{3/2}$ level should be lower in energy. Peaks B_i are a factor of 15 less intense than C_i, so we assign peak C to the $0 \leftarrow 0$ vibrational transition and peak B to the $v'=0 \leftarrow v''=1$ hot band transition. This yields a vibrational frequency of $539 \pm 10\ cm^{-1}$ for the anion $^2\Pi_u$ state. The electron affinity of Si_2 is given by the energy of peak C_1, 2.176 ± 0.002 eV.

There are several additional small peaks in Fig. 5 that we can assign. Peak c_2 lies $516\ cm^{-1}$ above peak C_2. This is very close to the vibrational frequency of the $X\,^3\Sigma_g^-$ state of Si_2 ($\nu = 509\ cm^{-1}$), and peak c_2 is therefore assigned to the $X\,^3\Sigma_g^-$ $(v'=1) \leftarrow {}^2\Pi_{1/2}(v''=0)$ transition. The partially resolved peaks c_1' and c_3' lie $528\ cm^{-1}$ to the red of peaks d_1 and d_3 and are separated by the same interval. Peaks c_1' and c_3' are therefore assigned to the $D\,^3\Pi_u$ $(v'=0) \leftarrow {}^2\Sigma_g^+$ $(v''=1)$ hot band transition, yielding $\nu_{01} = 528 \pm 10\ cm^{-1}$ for the anion $^2\Sigma_g^+$ state.

In is now clear that the energy level diagram of Fig. 7 is qualitatively correct. From our assignment, we conclude that the $^3\Pi_u$–$^3\Sigma_g^-$ gap in Si_2 is 83 ± 10 meV ($669 \pm 80\ cm^{-1}$) which is higher than Bauschlicher's prediction[9] but lower than in McLean's calculation.[12] For the anion, the $^2\Pi_u$ state is established as the ground state and the $^2\Sigma_g^+$–$^2\Pi^u$ splitting is only 25 ± 10 meV ($202 \pm 80\ cm^{-1}$). This is somewhat smaller than the values calculated by Bruna[20] and Raghavachari.[21]

The discussion so far has centered on peak positions. We obtain additional information from the peak intensities, namely, the bond lengths in the anion electronic states and

the anion vibrational temperature. This is possible because the bond lengths and frequencies for both the $X\,^3\Sigma_g^-$ and $D\,^3\Pi_u$ neutral states are known and the frequencies for the two anion states have been determined by our experiment. Consider first the $D\,^3\Pi_u \leftarrow {}^2\Sigma_g^+$ transition. Peaks e_i, d_i, and c_i' are nominally the $1\leftarrow 0$, $0\leftarrow 0$, and $0\leftarrow 1$ vibrational transitions associated with this electronic transition. In the absence of overlapping vibrational transitions, the e_i/d_i intensity ratio is proportional to the ratio of Franck–Condon factors for the $1\leftarrow 0$ and $0\leftarrow 0$ transitions, one could therefore extract the bond length in the anion $^2\Sigma_g^+$ state from the e_i/d_i ratio (assuming harmonic potentials throughout), and then obtain the anion vibrational temperature form the c_i'/d_i ratio.

In practice, some iteration is required in carrying out this procedure because the $2\leftarrow 1$ and $1\leftarrow 1$ sequence bands overlap the $1\leftarrow 0$ and $0\leftarrow 0$ transitions. Thus, in simulations of the spectrum, the e_i/d_i intensity ratio also depends on the assumed value of the anion vibrational temperature. In addition, peaks c_1' and c_3' are only partially resolved, so it is difficult to accurately determine their intensities. Our analysis yields a bond length of 2.116 ± 0.005 Å for the anion $^2\Sigma_g^+$ state and an approximate vibrational temperature of 500 K. A similar analysis of the $X\,^3\Sigma_g^- \leftarrow {}^2\Pi_u$ transition, using the known bond length of the $X\,^3\Sigma_g^-$ state and the c_2/C_2 intensity ratio gives $r_e = 2.207 \pm 0.005$ Å for the $^2\Pi_u$ state. This value of r_e along with a vibrational temperature of 500 K yields reasonable intensities for peaks B_1 and B_2. Our geometries for both $^2\Sigma_g^+$ and the $^2\Pi_u$ states agree very well with *ab initio* results on Si_2^-.[21] Figure 5 shows a simulation of the triplet band which includes all of the results discussed above.

From the C_1/C_2 (and B_1/B_2) ratio, we determine the $^2\Pi_{1/2}$,$^2\Pi_{3/2}$ population ratio to be 1/2, yielding a "spin–orbit temperature" of 125 K. Assuming the detachment cross sections out of the two spin–orbit states are the same, this result indicates that cooling of the spin–orbit states is more efficient than vibrational cooling in the cluster beam. This is a reasonable result as the energy interval is smaller for the spin–orbit states. All anion and neutral spectroscopic constants determined are summarized in Tables II and III.

The anion properties determined from the analysis of the triplet band enable the assignment of the higher energy transitions to the singlet states of Si_2. Figure 8 shows the one-electron transitions that can occur between the two anion electronic states and the $a\,^1\Delta_g$, $b\,^2\Pi_u$, $c\,^1\Sigma_g^+$, and $d\,^1\Sigma_g^+$ states of Si_2. In Fig. 10, we assume the dominant configuration for the $c\,^1\Sigma_g^+$ state to be the closed shell π_u^4 configuration and that for the $d\,^1\Sigma_g^+$ state to be the $\sigma_g^2\pi_u^2$ open shell configuration (see below). Only the $a\,^1\Delta_g \leftarrow {}^2\Pi_u$, $b\,^1\Pi_u \leftarrow {}^2\Sigma_u^+$, and $d\,^2\Sigma_g^+ \leftarrow {}^2\Pi_u$ neutral←anion transitions can occur by *s*-wave detachment and be observed in the threshold spectra. However, the $d\,^1\Sigma_g^+$ state is predicted to lie above the energy range of both photodetachment spectra.[11,12]

In all transitions to singlet states of the neutral, any doublet peaks observed in the threshold spectrum must represent transitions from the $^2\Pi_u$ state of the anion. We therefore assign the three equally spaced doublets between 480 and 454 nm in Fig. 6 to a vibrational progression in the $a\,^1\Delta_g \leftarrow {}^2\Pi_u$ electronic transition. The spacing between the doublets, $480 \pm 10\ cm^{-1}$, is the vibrational frequency of the $a\,^1\Delta_g$ state, while the splitting within each doublet is identical to the spin–orbit splitting in the anion $^2\Pi_u$ state determined from the triplet transitions. The $v' = 0 \leftarrow v'' = 0$ and

TABLE II. Spectroscopic constants for the first two electronic states of Si_2^-.

Si_2^- State	$\nu(cm^{-1})$	r_e(Å)	$A(cm^{-1})$	T_e(eV)
$^2\Sigma_g^+$	528 ± 10	2.116 ± 0.005	···	0.025 ± 0.010
$^2\Pi_u$	533 ± 5	2.207 ± 0.005	-122 ± 5	0

TABLE III. Spectroscopic constants for the first five electronic states of Si_2.

Si_2^- state	$\nu(cm^{-1})$	r_e(Å)	$A(cm^{-1})$	T_e(eV)
$X\,^3\Sigma_g^-$	509 ± 10	2.246	···	0
$D\,^3\Pi_u$	536 ± 5	2.115	-64 ± 10	$0.083 \pm .010$
$a\,^1\Delta_g$	486 ± 10	2.290 ± 0.010	···	$0.435 \pm .001$
$b\,^1\Pi_u$	540 ± 10	2.160 ± 0.005	···	$0.593 \pm .010$
$c\,^1\Sigma_g^+$	365[a]	2.16–2.31[a]	···	$0.637 \pm .010$

[a] References 18 and 19.

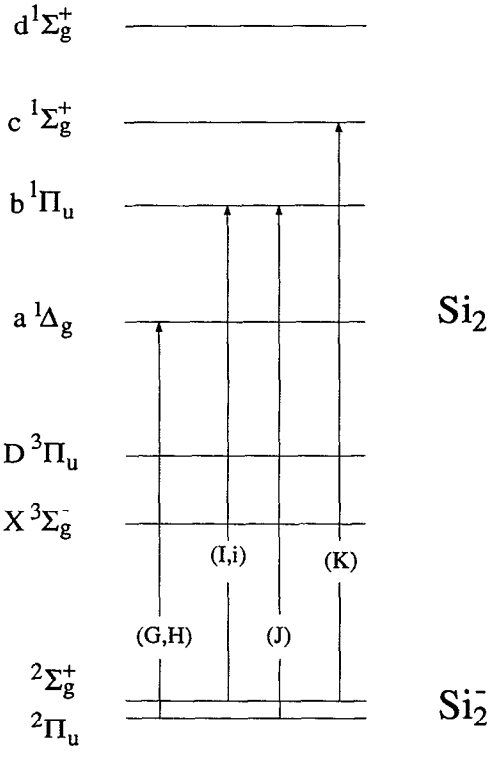

FIG. 8. Energy level diagram showing the electronic transitions between the $^2\Sigma_g^+$ and $^2\Pi_u$ electronic states of Si_2^- and the singlet electronic states of Si_2. The peaks in the spectra that correspond to each transition are shown in parentheses. The transition to the $d\,^1\Sigma_g^+$ state was not observed.

$1 \leftarrow 0$ doublets correspond to peaks G and H, respectively, in the photoelectron spectrum, while the smaller $2 \leftarrow 0$ doublet is not resolved in the photoelectron spectrum. This set of peaks represents the most extended vibrational progression seen in these spectra. Using the 2.207 Å bond length for the anion $^2\Pi_u$ state determined earlier, a Franck–Condon simulation similar to the one described above yields a bond length of 2.290 ± 0.010 Å for the $a\ ^1\Delta_g$ state. This is the first time the $a\ ^1\Delta_g$ state has been experimentally observed.

The threshold spectrum also shows two peaks, *I* and *i*, separated by $547 \pm 10\ cm^{-1}$. The remaining *s*-wave transition is the $b\ ^1\Pi_u \leftarrow {}^2\Sigma_u^+$ transition, and these two peaks are assigned to the $0 \leftarrow 0$ and $1 \leftarrow 0$ vibrational transitions associated with this electronic transition. Using our bond length and vibrational frequency for the anion $^2\Sigma_u^+$ state, we determine $R_e = 2.160 \pm 0.005$ Å for the $b\ ^1\Pi_u$ state. This value agrees well with the experimental value of Davis (2.16 Å);[19] he also found $\nu_{01} = 540\ cm^{-1}$ for the *b* state, which agrees with our results. This supports our assignment of these peaks as well as our bond length estimate for the anion $^2\Sigma_g^+$ state.

Peaks J, K, and L appear in the photoelectron spectrum but not the threshold spectrum and are most likely due to *p*-wave transitions. Peaks I and J are separated by only 20 meV, which corresponds to the anion $^2\Sigma_g^+ - {}^2\Pi_u$ splitting, so peak J is assigned to the $0 \leftarrow 0$ peak of the $b\ ^1\Pi_u \leftarrow {}^2\Pi_u$ transition. The transitions corresponding to peaks I and J involve removal of a π_u and σ_g electron, respectively, from the anion $^2\Pi_u$ state and are therefore analogous to peaks D and d in the triplet region. In accord with this, we note that the J/I and D/d intensity ratios show similar dependence on the laser polarization angle in the photoelectron spectra.

We next consider transitions to the $c\ ^1\Sigma_g^+$ and $d\ ^1\Sigma_g^+$ states of Si_2. Davis[19] found the $d\ ^1\Sigma_g^+ - b\ ^1\Pi_u$ splitting to be $4900\ cm^{-1}$ (0.608 eV), so transitions to the $d\ ^1\Sigma_g^+$ state would not appear in the 355 nm photoelectron spectrum (the TOF analyzer transmission is poor for $eKE < 0.3$ eV). Either peak K or L could be from a transition to the $c\ ^1\Sigma_g^+$ state, however. The question of whether the dominant MO configuration in the $c\ ^1\Sigma_g^+$ state is (a) π_u^4 or (b) $\sigma_g^2\pi_u^2$ has been raised in the *ab initio* studies of Bruna[11] and McLean.[12] If (b) were the case, then the $c\ ^1\Sigma_g^+$ state would be accessible by a one-electron transition only from the anion $^2\Pi_u$ state, and this can go by an *s*-wave. On the other hand, if π_u^4 were the dominant configuration, this state could be reached by a one-electron transition from the anion $^2\Sigma_g^+$ state by *p*-wave detachment. Peaks K and L are both absent in the threshold spectrum, which indicates they are both from *p*-wave detachment transitions. Assuming either K or L is a transition to the $c\ ^2\Sigma_g^+$ state, this implies that π_u^4 is the dominant MO configuration of the $c\ ^1\Sigma_g^+$ state, and that K or L is the $c\ ^1\Sigma_g^+ \leftarrow {}^2\Sigma_g^+$ transition.

Note that peak F in the triplet band was not assigned to any of the transitions in Fig. 7, and that it has the same dependence on laser polarization angle as peak L. This suggests that peaks F and L are due to transitions to different spin multiplets of the same Si_2 electronic state (F to the triplet, L to the singlet) and that peak K is the $c\ ^1\Sigma_g^+ \leftarrow {}^2\Sigma_g^+$ transition. This assignment is speculative, however, in that it is not clear what neutral $\leftarrow$ anion transition leads to peaks F and L.

We conclude by comparing the silicon dimer to the isovalent C_2 and SiC molecules. Just as in the case of the silicon dimer, a long standing controversy about the low-lying electronic states of C_2 was finally settled by Ballik and Ramsay,[41] establishing the $^1\Sigma_g^+$ $(\sigma_g^0\pi_u^4)$ as the ground state. The $^3\Pi_u$ and $^3\Sigma_g^-$ states were found to lie 0.089 eV and 0.798 eV above the ground state, respectively. It appears that C_2 is small enough to allow the π orbitals to interact very strongly leading to a ground state which maximizes π bonding. In the case of the SiC radical, Brazier *et al.*[42] report a 0.558 eV splitting between the $X\ ^3\Pi_u$ $(\sigma_g^1\pi_u^3)$ ground state and the $A\ ^3\Sigma_g^-$ $(\sigma_g^2\pi_u^2)$ first excited state, while the $^1\Sigma_g^+$ was found to be higher in energy than both of the triplet states. Thus, in SiC, for which the bond length is greater than C_2, the π orbital interaction has weakened while the σ orbitals are becoming important in stabilizing the molecule. Extrapolating from this trend, one expects σ bonding to have an even greater effect in the silicon dimer. Hence we expect the $^3\Sigma_g^-$ state to be the ground state, which agrees with the experimental results. The correlation of longer bond length with more σ bonding holds for all the Si_2 and Si_2^- electronic states; the σ^2 states ($^2\Pi_u$, $X\ ^3\Sigma_g^-$, $a\ ^1\Delta_g$) have longer bond lengths than the σ^1 states ($^2\Pi_u$, $D\ ^3\Pi_u$, $b\ ^1\Pi_u$).

CONCLUSION

Using negative ion photoelectron spectroscopy and threshold photodetachment, we have sorted out the low-lying electronic states in Si_2 and Si_2^-. The complexity of the electronic structure of this diatom indicates that the spectroscopy of larger Si clusters may be quite challenging. Nonetheless, the combination of the two techniques used in this work presents a promising approach to this problem. We have already obtained vibrationally resolved photoelectron spectra of Si_3^- and Si_4^-[43] and of several carbon cluster anions.[44] Measurements of the threshold photodetachment spectra of these clusters are in progress.

ACKNOWLEDGMENTS

This research is supported by the Office of Naval Research Chemistry Division and Young Investigator Program under Grant No. N0014-87-0485. We thank Krishnan Raghavachari and Celeste Rohlfing for communicating their Si_2^- results to us prior to publication.

[1] *Metal Clusters*, edited by M. Moskovits (Wiley, New York, 1986).
[2] M. D. Morse, Chem. Rev. **86**, 1049 (1986).
[3] *Physics and Chemistry of Small Clusters*, edited by P. Jena, B. K. Rao, and S. N. Kanna, NATO Advanced Science Institutes Series 158 (Plenum, New York, 1987).
[4] W. Weltner and R. J. Van Zee, Chem. Rev. **89**, 1713 (1989).
[5] K. Balasubramanian, Chem. Phys. Lett. **125**, 400 (1986).
[6] K. Raghavachari, J. Chem. Phys. **83**, 3520 (1985).
[7] G. Pacchioni and J. Koutecky, J. Chem. Phys. **84**, 3301 (1986); V. Bonacic-Koutecky, P. Fantucci, and J. Koutecky, *ibid.* **93**, 3802 (1990).
[8] H. Basch, Chem. Phys. Lett. **136**, 289 (1987).
[9] C. W. Bauschlicher, Jr. and S. R. Langhoff, J. Chem. Phys. **87**, 2919 (1987).
[10] K. Raghavachari, J. Chem. Phys. **84**, 5672 (1986).

[11]P. J. Bruna, S. D. Peyerimhoff, and R. J. Buenker, J. Chem. Phys. **72**, 5437 (1980).
[12]A. D. McLean, B. Liu, and G. S. Chandler, J. Chem. Phys. **80**, 5130 (1984).
[13]H. P. Lüthi and A. D. McLean, Chem. Phys. Lett. **135**, 352 (1987).
[14]F. Müller-Plathe and L. Laaksonen, Chem. Phys. Lett. **160**, 175 (1989).
[15]A. E. Douglas, Can. J. Phys. **33**, 801 (1955).
[16]I. Dubois and H. Leclercq, Can. J. Phys. **49**, 3053 (1971); D. E. Milligan, and M. E. Jacox, J. Can. Phys. **52**, 2594 (1969); R. D. Verma, and P. A. Warsop, Can. J. Phys. **41**, 152 (1963); A. Lagerqvist and C. Malmberg, Physica Scr. **2**, 45 (1970).
[17]M. R. Nimlos, L. B. Harding, and G. B. Ellison, J. Chem. Phys. **87**, 5116 (1987).
[18]I. Dubois and H. Leclercq, J. Phys. B **14**, 2807 (1981); Can. J. Phys. **49**, 3053 (1971).
[19]S. P. Davis and J. W. Brault, J. Opt. Soc. Am. B **4**, 20 (1987).
[20]P. J. Bruna, H. Dohmann, J. Anglada, V. Krumbach, S. D. Peyerimhoff, and R. J. Buenker, J. Mol. Struct. **93**, 309 (1983).
[21]K. Ragavachari and C. M. Rohlfing, J. Chem. Phys. **94**, 3670 (1991).
[22]J. Ho, K. M. Ervin, and W. C. Lineberger, J. Chem. Phys. **93**, 6987 (1990).
[23]O. Cheshnovsky, S. H. Yang, C. L. Pettiette, M. J. Craycraft, Y. Liu, and R. E. Smalley, Chem. Phys. Lett. **138**, 119 (1987).
[24]L. A. Posey, M. J. DeLuca, and M. A. Johnson, Chem. Phys. Lett. **131**, 170 (1986); L. A. Posey and M. A. Johnson, J. Chem. Phys. **88**, 5383 (1988).
[25]K. M. McHugh, J. G. Eaton, G. H. Lee, H. W. Sarkas, L. H. Kidder, J. T. Snodgrass, M. R. Manaa, and K. H. Bowen, J. Chem. Phys. **91**, 3792 (1989).
[26]G. Ganteför, M. Gausa, K. H. Meiwes-Broer, and H. O. Lutz, Z. Phys. D **9**, 253 (1988).
[27]D. G. Leopold, K. K. Murray, A. E. Stevens Miller, and W. C. Lineberger, J. Chem. Phys. **83**, 4849 (1985).
[28]R. B. Metz, A. Weaver, S. E. Bradforth, T. N. Kitsopoulos, and D. M. Neumark, J. Phys. Chem. **94**, 1377 (1990).
[29]T. N. Kitsopoulos, I. M. Waller, J. G. Loeser, and D. M. Neumark, Chem. Phys. Lett. **159**, 300 (1989).
[30]T. G. Dietz, M. A. Duncan, D. E. Powers, and R. E. Smalley, J. Chem. Phys. **74**, 6511 (1981); V. E. Bondybey, and J. H. English, *ibid.* **74**, 6978 (1981).
[31]W. C. Wiley and I. H. McLaren, Rev. Sci. Instrum. **26**, 1150 (1955).
[32]J. M. B. Bakker, J. Phys. E **6**, 785 (1972); **7**, 364 (1974).
[33]K. Müller-Dethlefs, M. Sander, and E. W. Schlag, Z. Naturforsch. Teil A **39**, 1089 (1984); Chem. Phys. Lett. **12**, 291 (1984); M. Sander, L. A. Chewter, K. Müller-Dethlefs, and E. W. Schlag, Phys. Rev. A. **36**, 4543 (1987).
[34]G. F. Gantefor, D. M. Cox, and A. Kaldor, J. Chem. Phys. **94**, 854 (1990).
[35]A preliminary analysis of the photoelectron spectra was presented in the MRS Proceedings, Fall 1990 Meeting.
[36]D. G. Leopold and W. C. Lineberger, J. Chem. Phys. **85**, 51 (1986).
[37]J. Cooper and R. N. Zare, J. Chem. Phys. **48**, 942 (1968).
[38]K. P. Huber and G. Herzberg, *Molecular Spectra and Molecular Structure IV, Constants of Diatomic Molecules* (Van Nostrand Reinhold, New York, 1979).
[39]E. P. Wigner, Phys. Rev. **73**, 1003 (1948).
[40]K. J. Reed, A. H. Zimmerman, H. C. Andersen, and J. I. Brauman, J. Chem. Phys. **64**, 1368 (1976).
[41]E. A. Ballik and D. A. Ramsay, Astrophys. J. **137**, 61, 84 (1963).
[42]C. R. Brazier, L. C. O'Brien, and P. F. Bernath, J. Chem. Phys. **91**, 7384 (1989).
[43]T. N. Kitsopoulos, C. J. Chick, A. Weaver, and D. M. Neumark, J. Chem. Phys. **93**, 6108 (1990).
[44]D. W. Arnold, T. N. Kitsopoulos, and D. M. Neumark (to be published).